

Experimental validation of a new adaptive control approach for a hybrid suspension system

Guido Koch, Sebastian Spirk, Enrico Pellegrini, Nils Pletschen and Boris Lohmann

Abstract—The paper presents the realization of a new suspension system and the experimental validation of a novel adaptive suspension control approach based on an adaptive reference model. The proposed “hybrid” suspension system includes a continuously variable hydraulic semi-active damper as well as an actuator in series to the suspension’s primary spring and can be realized based on stock hardware from production vehicles. The adaptive control approach emulates the dynamic behavior of a passive suspension system that is optimally tuned for the current driving state to maximize ride comfort while considering constraints on the dynamic wheel load and suspension deflection. Models of the actuators and the testrig are presented and the influence of actuator bandwidth on the suspension performance is analyzed. The measurements conducted on a quarter-car test rig confirm the significant performance potential of the proposed hardware combination and the adaptive control approach.

I. INTRODUCTION

Mechatronic suspension systems can ease the conflict of the objectives ride comfort, ride safety and limited suspension travel. In literature, fully active suspension systems with high bandwidth actuators being integrated between chassis and wheel mass have been intensively studied (see. e.g. [Hro97], [Ven93], [AH95], [FI04]). However, due to their high energy demand and cost aspects, in suspension systems of production vehicles primarily semi-active dampers are integrated, which are mainly controlled by skyhook based algorithms (see e.g. [JBE⁺08],[KCH74]). Low bandwidth systems with an actuator in series to the primary spring are integrated only in upperclass vehicles of *Mercedes Benz* [PSS03]. Although for the attenuation of the roll movement, semi-active and active systems are already combined, such a combination has not yet been employed for the vertical translatory movement of the chassis and wheel mass.

The combination of a continuously variable damper and a low bandwidth actuator has been studied theoretically in [SH87]. A more detailed analysis which takes into account realistic properties of the actuators and considers an adaptively controlled suspension system with time-varying controller parameters scheduled according to the driving state has been presented by the authors in [KFL]. It has been shown by means of an optimization based analysis that this adaptively controlled “hybrid” suspension system, containing active and semi-active actuators, can almost achieve the same performance as high-bandwidth suspension systems.

Corresponding adaptive controllers are presented e.g. in [LK97], [ZSG⁺08], [KDL08]. However, their implementabil-

ity is difficult since their parametrization is complex. In this context, the authors have proposed a transparent adaptive controller structure for the hybrid suspension configuration that takes into account nonlinearities of the suspension components and more detailed actuator models [KSL10]. The control concept emulates the behavior of a passive suspension system optimally tuned for the current driving state in terms of ride comfort and safety, i.e. it dynamically varies the stiffness and the damping of the suspension if necessary to keep the limits for the dynamic wheel load and the suspension deflection. It has been shown in simulations that the resulting performance of the adaptively controlled hybrid suspension configuration offers a significant performance potential at a lower demand of mechanical power compared to fully active suspension systems.

In this paper, the realization of a hybrid suspension strut and the experimental validation of its performance at a quarter-car test rig is presented. Based on models of the suspension and the actuators, the new adaptive reference model based controller structure is parametrized for the hybrid suspension. The realistic framework for the experiments is extended by using measurements of real road profiles as excitation signals. The proposed control approach is compared to skyhook based techniques in the experiments and it is analyzed, how the performance depends on the bandwidth of the actuator.

The remainder of the paper is organized as follows: The concept of the hybrid suspension is reviewed in Section II and the hardware realization is described. In Section III the model of the suspension system, the semi-active damper and the actuator controllers are presented. In Section IV, the application of the reference model based control approach for the hybrid suspension system is described and the corresponding experimental results are presented in Section V.

II. SUSPENSION CONCEPT

First, the concept of the hybrid suspension is briefly reviewed before its realization is presented in this Section. A quarter-car framework is considered (see e.g. [MW04]) and Figure 1 shows the models of a suspension with a semi-active damper (le.) and the hybrid suspension configuration (mid.), which additionally includes an actuator in series to the spring. The main idea for the control approach of the hybrid suspension system is the emulation of the dynamic behavior of a passive suspension system with time-varying stiffness and damping (Figure 1, right).

All Authors are with the Institute of Automatic Control, Technische Universität München, 86748 Garching, Germany
guido.koch@mytum.de

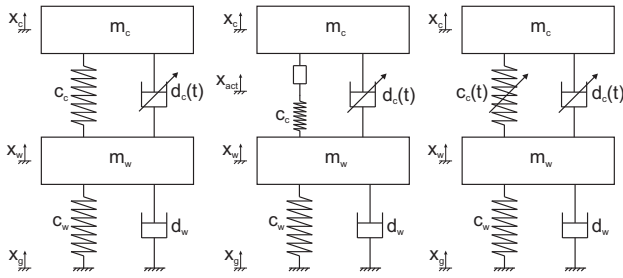


Fig. 1. Quarter-car models of the semi-active, the hybrid and the time-varying passive reference suspension model.

A. System requirements

The system requirements considered here are similar to the ones presented in [KSL10]. However, the constraints are adjusted to the parameters of the real suspension system that is used for the experiments.

- The root mean square (rms) value of the vertical chassis acceleration $\|\ddot{x}_c\|_{\text{rms}}$ should be minimized, especially in the frequency range where the human body is most sensitive for vertical mechanical vibrations (4 – 8 Hz) [ISO97]. To quantify ride comfort, the comfort index $\|\ddot{x}_{c,\text{comf}}\|_{\text{rms}}$ is considered, which results from \ddot{x}_c after filtering with the comfort filter given in [ISO97].
- The rms-value of the dynamic wheel load $F_{\text{dyn}}(t)$ that depends on the tire stiffness and damping, i.e. $F_{\text{dyn}}(t) = f_{F_{\text{dyn}}}(x_w - x_g, \dot{x}_w - \dot{x}_g)$, should be bounded by

$$\max(\|F_{\text{dyn}}\|_{\text{rms}}) \leq \frac{(m_c + m_w)g}{3} = \frac{F_{\text{stat}}}{3}, \quad (1)$$

where g denotes the gravitational constant and F_{stat} is the static wheel load (see [MW04]).

- The suspension deflection $x_{cw} = x_c - x_w$ is limited to $\underline{x}_{cw} = -0.1\text{m}$ in compression and to $\bar{x}_{cw} = 0.11\text{m}$ in rebound direction of the spring. Furthermore, it is noted that due to the asymmetric damping characteristic and the resulting dynamic change of the equilibrium position of the passive suspension system the standard deviation $\|x_c - x_w\|_{\text{std}}$ is considered for the performance analysis of the suspension.
- The hydraulic actuator's displacement Δx_{hy} is limited to $\pm 4\text{cm}$. The maximum spread of the integrated semi-active damper is illustrated in Figure 4.
- Minimum power demand of the hydraulic actuator is intended, which is quantified by the rms-value of the positive mechanical actuator power

$$\|P^+\|_{\text{rms}} = \sqrt{\frac{1}{T} \int_0^T (P^+)^2(\tau) d\tau}, \quad (2)$$

$$P^+(t) = \begin{cases} F(t)\Delta\dot{x}_{hy}(t) & \text{for } F(t)\Delta\dot{x}_{hy}(t) > 0 \\ 0 & \text{else,} \end{cases} \quad (3)$$

since in the considered application the spring operates only in compression. For a more realistic analysis of the absolute power demand, the hydraulic efficiency factors have to be taken into account. However, since

these factors are not exactly known for the application at hand and a relative comparison of power demand is intended (as in [KSL10]), the approach represents a suitable method for the power demand analysis.

B. Realization of a hybrid suspension

In order to provide a realistic framework for the design of the hybrid suspension system, it is realized as a combination of hardware components from production vehicles (Figure 2): A modern continuously variable hydraulic damper from the *BMW 7 Series* (model year 2009) and a hydraulic suspension actuator integrated in series to the primary spring from the *Active Body Control System (ABC)* of a *Mercedes SL Roadster* (model year 2003) (see also [PSS03]). The damping is individually adjustable in pressure and rebound direction by two external valves.

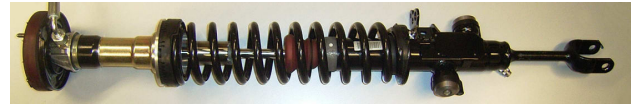


Fig. 2. Realization of the hybrid suspension

C. Quarter-car test rig

The test rig used for the experiments is shown in Figure 3. It is designed using parameters of the *BMW 7 series* (model year 2009), which represents an upperclass vehicle. The sprung mass is $m_c = 507\text{kg}$ and the unsprung mass is $m_w = 68\text{kg}$. A highly dynamic hydraulic actuator is used to excite the tire vertically simulating the road excitation. The measurement signals used for suspension control at

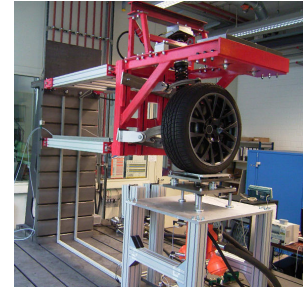


Fig. 3. Quarter-car test rig for the experiments.

the test rig are the accelerations \ddot{x}_c , \ddot{x}_w , the suspension deflection $x_c - x_w$, the deflection of the suspension actuator Δx_{hy} , the pressure inside the suspension actuator p_c and the damper valve currents for rebound and compression $\mathbf{i}_d = [i_{d,c} \ i_{d,r}]^T$. Most of the employed sensors are taken from the original vehicles. Moreover, the dynamic wheel load F_{dyn} and the road displacement x_g are measured for the performance evaluation of the mechatronic suspension.

III. MODELING

Since the authors have received parts of the suspension component data from an industry partner, numerical values of the corresponding parameters are omitted.

A. Suspension modeling

In many works the tire dynamics are represented by a linear spring since the tire damping is small compared to the damping of the suspension. In order to demonstrate the possibility of the handling of nonlinearities by the proposed control approach, a more detailed tire model is employed in this study, i.e. a Gehmann-Model [MW04]. The Gehmann-Model represents the tire as a parallel connection of a spring and a series connection of a spring and a damper.

The kinematics of the considered double wishbone suspension are mainly defined by the geometry of wishbone struts and the inclined assembly of the suspension strut. Due to the change of the inclination of the suspension strut during suspension deflection, the kinematic transmission factor (see e.g. [Mat07]) $i(t) = f_i(x_c(t) - x_w(t))$ changes linearly with the suspension deflection. The primary spring is a steel spring with a linear characteristic. Moreover, additional buffers are integrated into the suspension strut to provide softer endstops. Thus, the resulting suspension force deflection characteristic becomes progressive when the suspension operates in a range where the buffers are compressed. Coulomb friction effects in the suspension struts have been identified experimentally and are taken into account for the modeling.

The described models of the tire, the suspension kinematics and friction effects are integrated into a quarter-vehicle model for the modeling of the complete suspension setup. As in [KSL10], the state-vector \mathbf{x} and the output vector \mathbf{y} are introduced as

$$\mathbf{x} = [x_c - x_w, \dot{x}_c, x_w - x_g, \dot{x}_w]^T, \quad (4)$$

$$\mathbf{y} = [\ddot{x}_c, F_{dyn}, x_c - x_w]^T. \quad (5)$$

With the control input of the actuator $u_{hy}(t) = \Delta x_{hy} = i(t)(x_c(t) - x_{act}(t))$ and the semi-active damper $u_{cvd}(t) = F_d(t)$ as well as the disturbance input $u_d(t) = \dot{x}_g(t)$, the quarter-car model of the hybrid vehicle suspension system can be expressed as a fourth order state space model in the form.

$$\dot{\mathbf{x}}(t) = \mathbf{f}(\mathbf{x}(t), u_{hy}(t), u_{cvd}(t), u_d(t)), \quad (6)$$

$$\mathbf{y}(t) = \mathbf{g}(\mathbf{x}(t), u_{hy}(t), u_{cvd}(t), u_d(t)). \quad (7)$$

B. Actuator models and control

Actuator models are required for the simulation and for the design of tracking controllers for $u_{hy}(t)$ and $u_{cvd}(t)$, respectively.

1) *Hydraulic actuator*: A detailed nonlinear model similar to the one presented in [AH95] is used for the parametrization of the actuator controller structure, which involves feedforward control for the actuator velocity as well as a PI-feedback controller for the actuator position. The control valve of the actuator offers a higher bandwidth than the stock component of the vehicle and in order to be able to compare the influence of different bandwidths of the controlled actuator, a first order low pass filter is used for the reference signals for the actuator position and velocity. The default cutoff frequency of the lowpass filter is $f_c = 5$ Hz

as this represents the bandwidth of the original *ABC-system* [PSS03].

2) *Continuously variable damper*: The static behavior of the semi-active damper is modeled by its nonlinear characteristic that relates the damper relative velocity $\dot{x}_c - \dot{x}_w$ and the valve currents \mathbf{i}_d to the damper force F_d . The damper dynamics are taken into account as proposed in [KSL10] using two transfer functions

$$G_{el}(s) = \frac{1}{1 \cdot 10^{-3}s + 1} \quad \text{and} \quad G_m(s) = \frac{1}{10 \cdot 10^{-3}s + 1}, \quad (8)$$

which describe the electrical (input: voltage input of power electronic unit; output: valve currents \mathbf{i}_d) and the mechanical dynamics (input: commanded damper force $F_{d,c}$; output: actual damper force F_d). It is noted that the time constants in (8) have been identified experimentally and are slightly different from the ones published in [KSL10]. If $\mathbf{i}_d = [0 \ 0]^T$, the hardest damping characteristic is activated.

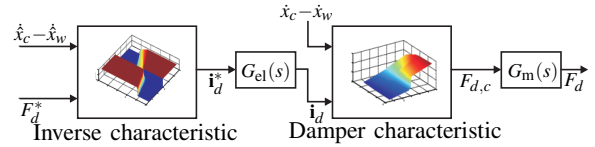


Fig. 4. Damper model and feedforward control [KSL10].

For the control of the damper an estimate of the relative damper velocity \hat{x}_{cw} is utilized that is obtained from the measurements of \dot{x}_c , \dot{x}_w and $x_c - x_w$ [KKL10], [KSL10]. To calculate the reference current i_d^* from the reference force F_d^* a simple feedforward prefiltering approach using an inversion of the static damper characteristic is employed (see Figure 4) since the actual damper force is not measured and the electrical time constant is small. The tracking control of the desired damper current is accomplished by an internal PI-controller of the power electronic unit.

IV. ADAPTIVE REFERENCE MODEL BASED CONTROL

The adaptive reference model based controller structure is depicted in Figure 5. In the following, the focus is primarily on implementation aspects but first the idea of the control approach (based on [KSL10]) is reviewed.

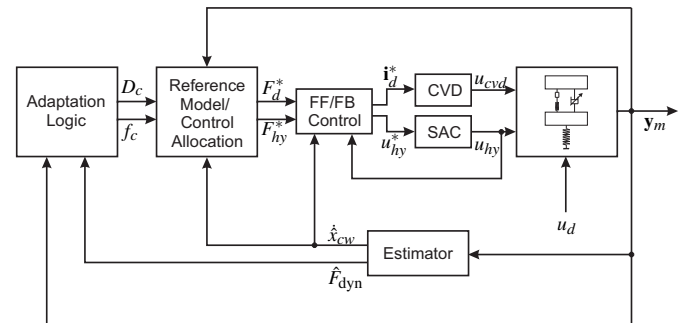


Fig. 5. Adaptive reference model based controller structure for the hybrid suspension system.

The control approach emulates the dynamic behavior of a time-varying reference model, which is a passive suspension system that is optimally tuned for the current driving state. Optimality in this context refers to minimum rms-values of the vertical chassis acceleration while the limits for the dynamic wheel load and suspension deflection are not violated. Therefore, the driving state is determined by an adaptation logic, which uses an estimate of the dynamic wheel load \hat{F}_{dyn} and the suspension deflection measurement and maps their rms-values (over a time interval of approx. 2sec) as well as rapid changes of these quantities to two real scheduling parameters q_{fdyn} and q_{susp} , both ranging in the interval $0 \leq q_i \leq 2$ (see [KSL10], [KDL08] for more details on the adaptation logic and [KKL10] for details on the filter based estimation). If their values equal zero, a comfort oriented passive suspension configuration with low chassis eigenfrequency and damping ratio is emulated. For $q_i > 0$ the controller increases the damping and eventually “stiffens” the suspension characteristic.

The optimal resulting damping and spring forces are calculated as shown in Figure 6 from the optimal undamped natural frequency of the sprung mass $f_c(t) = \frac{1}{2\pi} \sqrt{\frac{c_c(t)}{m_c}}$ and its damping ratio $D_c(t) = \frac{d_c(t)}{2\sqrt{c_c(t)m_c}}$, that have been determined by the adaptation logic. The passive suspension model includes the nonlinear dynamic behavior resulting from the spring characteristic, friction effects of the suspension and the damper as well as the kinematic effects. The result of this control approach is that the passive suspension forces are compensated and the reference force signals of the adaptive reference model are tracked.

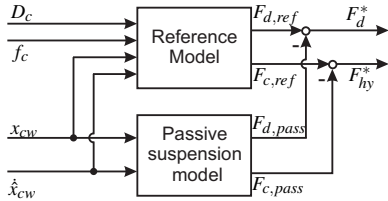


Fig. 6. Reference model based control force calculation ($F_{c,j}$ represents a spring force, $F_{d,j}$ represents a damper force).

The reference model and the adaptation laws are derived in simulations from carpet plots (“conflict diagrams”) relating the quantities $\|\ddot{x}_{c,comf}\|_{rms}$, $\|F_{dyn}\|_{rms}$ and $\|x_c - x_w\|_{std}$ for variations of suspension parameters [Hro97]) of the passive suspension configuration with varying stiffness and damping. For the calculation of the carpet plots a passive quarter-car model including a linear primary spring, the Gehmann-model of the tire and friction effects is employed. The damper characteristics has been linearized separately in compression and rebound direction (at $\dot{x}_{cw} = \pm 0.58 \frac{m}{sec}$) using the damper current representing the passive reference, so that a piecewise linear damping and a linear spring stiffness is used in the reference model. The damping ratio is calculated as the mean value of both linear damping coefficients (see e.g. [MW04]). To vary the damping ratio, the piecewise linear damping

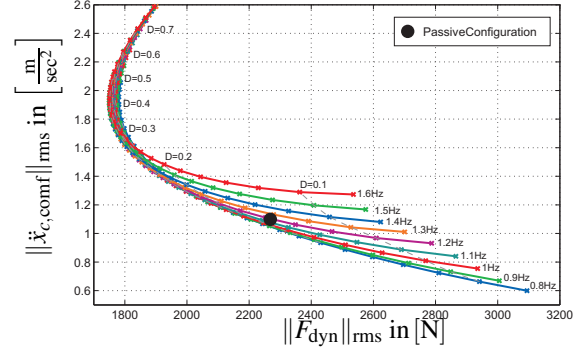


Fig. 7. Carpet plot for passive suspension system with different f_c and D_c (for stochastic road model).

characteristic of the reference model is scaled accordingly.

The original passive suspension setting has a damping ratio of the chassis mass of $D_{c,p} = 0.21$ and a corresponding natural frequency of $f_{c,p} = 1.10\text{Hz}$. The reference model that is used for the adaptive controller can vary these quantities in the ranges $0.18 \leq D_c \leq 0.7$ and $0.8\text{Hz} \leq f_c \leq 1.6\text{Hz}$. The Pareto-fronts depicted in Figure 7 are used to formulate driving state dependent adaptation laws as is described in Section IV-A.

Major differences of the proposed control approach compared to variants of model reference adaptive control methods for vibration control applications proposed in literature (see e.g. [SCH91], [ZSN05]) are that the reference model is time-varying and it is based on the well-known dynamics of passive suspension systems rather than skyhook concepts.

A. Adaptation laws

The optimal values of the parameters f_c and D_c are gained from the Pareto-fronts of the carpet plots of the reference model (Figure 7 depicts the carpet plot visualizing the Pareto-front for the conflict between ride comfort and ride safety). These optimal parameters are mapped to the scheduling parameters q_{fdyn} and q_{susp} so that adaptation laws to achieve the desired values for f_c and D_c for every driving state can be formulated (Figure 8). As can be seen, the low natural frequency should be maintained as long as the driving state permits and the adaptation is first realized by adjusting the damping ratio. Depending on the suspension deflection, a minimum damping ratio $D_{c,min}$ and a minimum $f_{c,min}$ are calculated, which dominate the wheel load optimal settings.

B. Control Allocation

The increase of the natural frequency f_c by a change of the spring stiffness requires an active element, the damping ratio $D_c(t)$ can be adjusted by the semi-active damper. Consequently, the reference forces for the hydraulic actuator F_{hy}^* are calculated from f_c and the damper force F_d^* results from D_c . Furthermore, the tracking error of the hydraulic actuator is added to the reference force of the damper in order to ease the effect of the actuator’s bandwidth limitation.

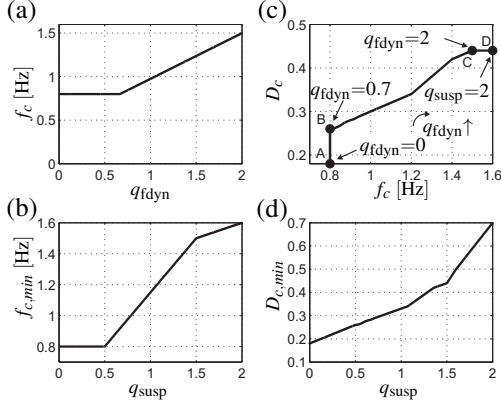


Fig. 8. Reference model based adaptation laws.

Consequently, the force reference values are calculated as

$$F_{hy}^* = (m_c(2\pi f_c)^2 - c_{c,pass}(\mathbf{x}))x_{cw}, \quad (9)$$

$$F_d^* = (4\pi f_c m_c D_c - d_{c,pass}(\mathbf{x}))\dot{x}_{cw} + (F_{hy}^* - F_{hy}). \quad (10)$$

In [KSL10] a method has been presented to guarantee uniform asymptotic stability of the closed loop suspension system by a switching restriction for the virtual stiffness of the suspension emulated by the hydraulic actuator.

V. EXPERIMENTAL VALIDATION AT THE QUARTER-CAR TEST RIG

The experiments are conducted using two measurements of real road profiles as excitation signals. The road profiles represent a bad highway road profile (P1) as well as a country road (P2). While profile 1 is more challenging regarding suspension deflection, profile 2 contains more high frequency components, which makes it more challenging to provide ride comfort despite limiting the wheel load variations.

To evaluate the performance results of the hybrid suspension and the proposed control approach, a skyhook damping control law and an adaptive skyhook algorithm (see [KCH74], [HSH02]) are utilized as benchmarks. The benchmark concepts are used for the semi-active suspension configuration (SA-Skyh., SA-Ad.) and the active configuration (Act.-Skyh.), in this case with a fixed setting of the semi-active damper. The reference damping force in the adaptive case is

$$F_{d,sky} = -d_{sky}\dot{x}_c - \left(d_{c,c} + (d_{c,s} - d_{c,c}) \frac{q_{fdyn}}{2} \right) \dot{x}_{cw}, \quad (11)$$

with the damping terms $d_{c,c} = 300 \frac{\text{Nsec}}{\text{m}}$ (comfort damping), $d_{c,s} = 1416 \frac{\text{Nsec}}{\text{m}}$ (safety damping) and $d_{sky} = 2000 \frac{\text{Nsec}}{\text{m}}$. The damping parameters of the skyhook benchmark controllers are obtained by means of optimization to minimize the rms-values $\|\dot{x}_{c,comf}\|_{\text{rms}}$ and lower $\|F_{dyn}\|_{\text{rms}}$ as long as the constraint given by the suspension deflection limits permits. For the nonadaptive skyhook damping, $q_{fdyn} = 0$ holds in (11). If the skyhook algorithms are applied for the semi-active system, the force $F_{d,s}$ can only be generated by the damper if the skyhook condition $\dot{x}_c(\dot{x}_c - \dot{x}_w) \geq 0$ is fulfilled and $F_{d,s}$ is reachable by the damper characteristic, otherwise the force is clipped by the damper.

A. Measurement results

Spider charts are used to visualize the performance gain

$$PG(\|\cdot\|) = 1 - \frac{\|\cdot\|_{\text{controlled}}}{\|\cdot\|_{\text{passive}}} \quad (12)$$

for each considered quantity $\|\cdot\|$ (see Section II-A) with respect to the passive suspension. A positive value of $PG(\|\cdot\|)$ denotes a reduction of the absolute value of the corresponding quantity and thus a performance improvement. Figure 9 summarizes the results for the measurements of the benchmark systems and the hybrid suspension for both road profiles. The grey line denotes the performance of the passive suspension and the numerical values for profile 1 are summarized in Table I (with a 5 Hz actuator bandwidth).

TABLE I
EXPERIMENTAL RESULTS FOR PROFILE 1

Quantity	Passive	SA-Skyh.	SA-Ad.	Act-Skyh.	Hybrid
$\ \dot{x}_c\ _{\text{rms}}$ in $\frac{\text{m}}{\text{sec}^2}$	1.88	1.65	1.58	1.50	1.24
Benefit vs. pass.	-	12%	16%	20%	34%
$\ \dot{x}_{c,comf}\ _{\text{rms}}$ in $\frac{\text{m}}{\text{sec}^2}$	1.24	1.18	1.01	1.08	0.87
Benefit vs. pass.	-	5%	19%	13%	30%
$\ F_{dyn}\ _{\text{rms}}$ in N	1136	1027	1078	1009	1016
Benefit vs. pass.	-	10%	5%	11%	11%
$\min(F_{dyn})$ in N	-3479	-2918	-3206	-2876	-2979
Benefit vs. pass.	-	16%	8%	17%	14%
$\min(x_c - x_w)$ in cm	-7.7	-6.2	-6.6	-6.4	-7.6
Benefit vs. pass.	-	19%	14%	18%	1%
$\ P^+\ _{\text{rms}}$ in W	0	0	0	92	115

In order to study the influence of the bandwidth of the hydraulic actuator, the bandwidth of the filter for the reference signal of the actuator controller is increased from 5 Hz to 12 Hz. The resulting slightly higher performance is visualized in Figure 9. This comes, however, at the price of a higher power demand (for profile 1 the increase is $\Delta\|P^+\|_{\text{rms}} = 60 \text{ W}$). Consequently, $\omega_c = 2\pi 5 \text{ Hz}$ (the bandwidth of the ABC) represents a good trade-off for the hydraulic actuator. As can be seen in Figure 9, the adaptive reference model based control approach in combination with the hybrid suspension configuration outperforms the benchmark controllers by far. The measurement results confirm that the presented approach eases the inherent conflict of suspension systems by offering performance advantages for ride comfort and ride safety simultaneously. The performance gains of the hybrid suspension come along with higher suspension deflections (especially in the case of the higher actuator bandwidth), which is not a drawback since the adaptation logic prevents hitting the suspension limits.

For profile 2, which contains more high frequency components, the performance can also be increased by the hybrid suspension, however, by permitting higher dynamic wheel loads and suspension deflection (both quantities are still well within the formulated limits). Due to this property of the road excitation signal, the actuator becomes less involved which reduces the actuator power to $\|P^+\|_{\text{rms}} = 60 \text{ W}$. Thus, the

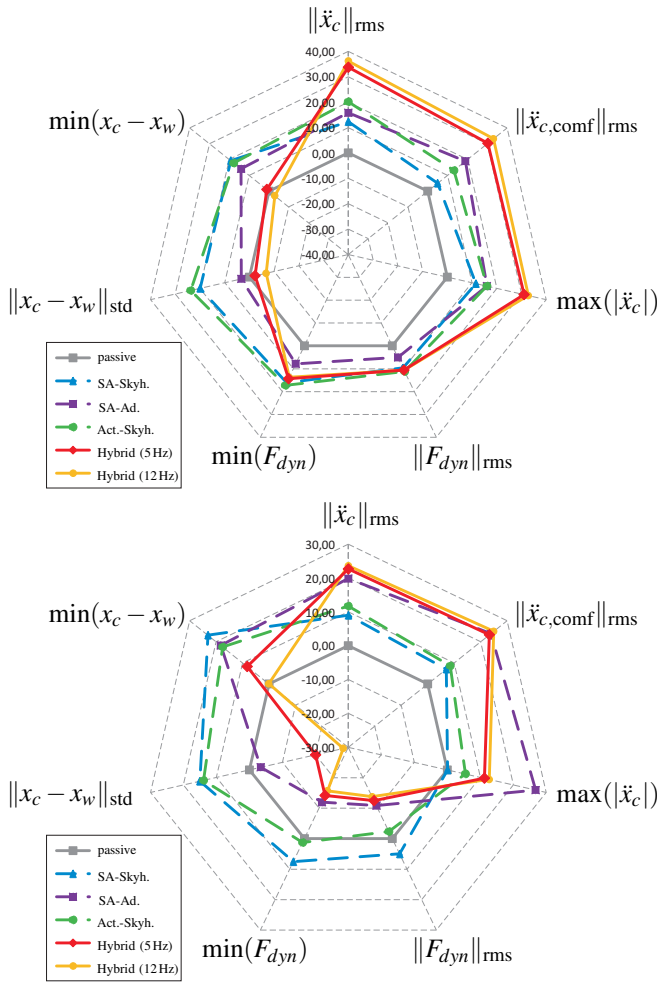


Fig. 9. Controller performance for profile 1 with $v_{p1} = 50 \frac{\text{km}}{\text{h}}$ (upper) and profile 2 with $v_{p2} = 30 \frac{\text{km}}{\text{h}}$ (lower) for different actuator bandwidths $\omega_c = 2\pi 5\text{Hz}$, $\omega_c = 2\pi 12\text{Hz}$.

ride comfort for profile 2 can obviously also be increased considerably by the controlled semi-active damper using the proposed adaptive skyhook algorithm (see (11)).

In order to show the full potential of the proposed control approach, the velocity for passing profile 1 is increased to $75 \frac{\text{km}}{\text{h}}$. Simulations have shown that the wheel would loose contact to the road with the conventional passive damping ratio ($D_{c,p} = 0.21$). Thus, the damping ratio of the passive system is increased to $D_{c,p} = 0.42$. Neither wheel load nor suspension deflection limits are violated by both configurations in the experiments but the performance increase by the hybrid configuration is 36% regarding ride comfort while $\|F_{dyn}\|_{rms}$ remains almost unchanged.

VI. CONCLUSION AND OUTLOOK

A realization of a hybrid suspension configuration based on actuator components from production vehicles has been presented in the paper. The hybrid suspension strut has been integrated into a quarter-car test rig and using this setup, its performance capability in combination with an adaptive reference model based control approach has been validated in

a very realistic framework. The performance comparison has been conducted with respect to established control concepts (skyhook based techniques) and the experimental results have underlined the performance potential not only of the proposed new adaptive suspension control concept but for adaptive suspension control in general. Future work will involve the analysis of alternative reference model structures.

REFERENCES

- [AH95] A. Alleyne and J. K. Hedrick. Nonlinear Adaptive Control of Active Suspensions. *IEEE Transactions on Control Systems Technology*, 3:94 – 101, 1995.
- [FI04] D. Fischer and R. Isermann. Mechatronic semi-active and active vehicle suspensions. *Control Engineering Practice*, 12:1353 – 1367, 2004.
- [Hro97] D. Hrovat. Survey of advanced suspension developments and related optimal control applications. *Automatica*, 33(10):1781–1817, 1997.
- [HSH02] K.-S. Hong, H.-C. Sohn, and J. K. Hedrick. Modified skyhook control of semi-active suspensions: A new model, gain scheduling, and hardware-in-the-loop tuning. *Journal of Dynamic Systems, Measurement, and Control*, 124:158 – 167, 2002.
- [ISO97] ISO. *ISO 2631-1:1997 - Mechanical vibration and shock - Evaluation of human exposure to whole-body vibration*. International Organization for Standardization, 1997.
- [JBE⁺08] M. Jautze, A. Bogner, J. Eggendinger, G. Rekewitz, and A. Stumm. Das Verstelldämpfersystem Dynamische Dämpfer Control. *ATZ extra, Der neue BMW 7er*:100–103, 2008.
- [KCH74] D. Karnopp, M. J. Crosby, and R. A. Harwood. Vibration control using semi-active force generators. *ASME Journal of Engineering for Industry*, 96:619–626, 1974.
- [KDL08] G. Koch, K. J. Diepold, and B. Lohmann. Multi-objective road adaptive control of an active suspension system. In H. Ulbrich and L. Ginzinger, editors, *Motion and Vibration Control*, pages 189 – 200. Springer, 2008.
- [KFL] G. Koch, O. Fritsch, and B. Lohmann. Potential of low bandwidth active suspension control with continuously variable damper. *To appear in Control Engineering Practice*.
- [KKL10] G. Koch, T. Kloiber, and B. Lohmann. Nonlinear and filter based estimation for vehicle suspension control. In *Proc. of the 49th IEEE Conference on Decision and Control*, 2010.
- [KSL10] G. Koch, S. Spirk, and B. Lohmann. Reference model based adaptive control of a hybrid suspension system. *Proceedings of the IFAC Symposium Advances in Automotive Control*, 2010.
- [LK97] J. Lin and I. Kanellakopoulos. Nonlinear design of active suspensions. *IEEE Contr. Syst. Mag.*, 17:45–59, 1997.
- [Mat07] W. Matschinsky. *Radführungen der Strassenfahrzeuge - Kinematik, Elasto-Kinematik und Konstruktion*. Springer, 2007.
- [MW04] M. Mitschke and H. Wallentowitz. *Dynamik der Kraftfahrzeuge*. Springer, Berlin, 2004.
- [PSS03] M. Pyper, W. Schiffer, and W. Schneider. *ABC - Active Body Control*. Verlag Mod. Ind., Augsburg, 2003.
- [SCH91] M. Sunwoo, K. C. Cheok, and N. J. Huang. Model reference adaptive control for vehicle active suspension systems. *IEEE Transactions on industrial electronics*, 38(3):217 – 222, 1991.
- [SH87] R. S. Sharp and S. A. Hassan. On the Performance of Active Automobile Suspension Systems of Limited Bandwidth. *Vehicle System Dynamics*, 16:213–225, 1987.
- [Ven93] P. J. Th. Venhovens. *Optimal Control of Vehicle Suspensions*. PhD thesis, Delft University of Technology, Faculty of Mechanical Engineering, 1993.
- [ZSG⁺08] A. Zin, O. Sename, P. Gaspar, L. Dugard, and J. Bokor. Robust LPV- \mathcal{H}_∞ control for active suspensions with performance adaptation in view of global chassis control. *Veh. Syst. Dyn.*, 46(10):889–912, 2008.
- [ZSN05] L. Zuo, J.-J. E. Slotine, and S. A. Nayfeh. Model reaching adaptive control for vibration isolation. *IEEE Transactions on Control Systems Technology*, 13(4):611 – 617, 2005.